history of Mount St. Helens, it was predicted that the volcano was likely to erupt, possibly before the end of this century (*10*). The early activity observed at Mount St. Helens is similar in character to the eruption of Lassen Peak Volcano in California during the period 1914 to 1921 (*11*). During the first year of Lassen's activity, approximately 150 phreatic eruptions sent cold ash and steam columns to heights as great as 3000 m above the crater. No report was made of sulfur or acid fumes during that period. Magmatic activity began on 19 May 1915 with a violent pyroclastic eruption of dacitic magma. Nuée ardente–type eruptions followed on 20 and 22 May. Then the eruptive activity subsided with minor periods of heightened activity, until at least February 1921. Our observations of Mount St. Helens are certainly consistent with the possibility that the current eruptive style may evolve into eruptions with a larger magmatic component.

Volcanic gas geochemistry can provide indications of increasing magmatic contributions to eruptions. At Mount Etna in Sicily, the rate of release of SO$_2$ has been shown to increase before magmatic eruptions (*12*). The S/Cl ratio in leachates is related to SO$_2$/HCl ratios in volcanic gas (*13*). Monitoring the SO$_2$ emission and measuring the S/Cl ratio in leachates could provide important premonitory indicators of a magmatic eruption. Therefore, continued geochemical monitoring of Mount St. Helens is advised.

RICHARD E. STOIBER
STANLEY N. WILLIAMS
LAWRENCE L. MALINCONICO
Department of Earth Sciences,
Dartmouth College,
Hanover, New Hampshire 03755

References and Notes

1. D. Mullineaux *et al.*, *Sci. Event Alert Network Bull.* **5** (No. 3), 2 (1980).
2. *Oregon Journal* (29 March 1980), p. 1.
3. R. E. Stoiber and A. Jepsen, *Science* **182**, 577 (1973).
4. We use the term "rate" to indicate the mass that would be emitted if the volcano were erupting continuously. In fact, the eruptive periods at Mount St. Helens probably totaled less than 1/10 of a day.
5. R. E. Stoiber, G. B. Malone, G. P. Bratton, *Geol. Soc. Am. Program Abstr.* **10**, 480 (1978).
6. P. Taylor and R. E. Stoiber, *Geol. Soc. Am. Bull.* **84**, 1031 (1973).
7. W. I. Rose, Jr., *Geology* **5**, 621 (1977).
8. Data in Table 1 are from volcanic eruptions that represent a variety of these variables, although all combinations of all variables are not included in any one sample set.
9. S. Thorarinsson, in *Volcanic Activity and Human Ecology*, P. D. Sheets and D. K. Grayson, Eds. (Academic Press, New York, 1979), pp. 125–156.
10. D. R. Crandell, D. R. Mullineaux, M. Rubin, *Science* **187**, 438 (1975); D. R. Crandell and D. R. Mullineaux, *U.S. Geol. Surv. Bull. 1383-C* (1978).
11. A. L. Day and E. T. Allen, *The Volcanic Activity and Hot Springs of Lassen Peak* (Publication 360, Carnegie Institution of Washington, Washington, D.C., 1925).
12. L. Malinconico, *Nature (London)* **276**, 112 (1979).
13. W. I. Rose, Jr., R. E. Stoiber, L. Malinconico, in *Orogenic Andesites and Related Rocks*, R. Thorpe, Ed. (Wiley, New York, in press).
14. The first sample was collected by D. Swanson (USGS) and made available to us by T. Casadevall (USGS). The second sample was collected by L.L.M. with logistical support provided by a USGS helicopter and D. A. Johnston (USGS).
15. The assistance of D. Burrington of NBC News and T. Casadevall and D. A. Johnston of the USGS and the cooperation of the USGS personnel in Vancouver, Wash., are gratefully acknowledged. This research was supported under NASA Cooperative Agreement 5-22.

21 April 1980; revised 14 May 1980

Contact Metamorphism by an Ophiolite Peridotite from Neyriz, Iran

Abstract. *Ophiolites are conventionally regarded as fragments of former oceanic lithosphere. Mineralogical and field evidence indicates that peridotite of the Neyriz ophiolite was intruded at high temperature into folded crystalline limestones, forming skarns. This excludes the formation of the ophiolite at a mid-ocean ridge but is consistent with its origin by intrusion during continental rifting.*

Basic and ultrabasic rocks of an ophiolite complex are exposed in the Neyriz region of southern Iran where they were emplaced by thrusting during the late Cretaceous (*1*). One unusual aspect of this ophiolite is the presence of skarns at the contact between crystalline limestones and the ophiolite peridotite. These skarns have been interpreted (i) as remnants of an intrusive contact of prethrusting (*1, 2*) or postthrusting (*3*) age, (ii) as the product of metamorphism at the base of an obducted ophiolite (*4*), or (iii) as the result of fortuitous association with the ophiolite during subduction (*5*). The mineral assemblages reported (*1*) suggest other possible origins, such as calcium metasomatism associated with serpentinization or regional metamorphism of impure limestones. The origin of these skarns is critical to the interpretation of the Neyriz ophiolite and the evolution of the Zagros mountain chain and they are of more general interest as ophiolite-related metamorphic rocks, yet their detailed mineralogy is unknown. I report mineralogical data from new skarn localities that indicate contact metamorphism of limestone by the ophiolite peridotite.

Mountain-size marble blocks are exposed just east of Tang e Hana, a small village 30 km northwest of Neyriz. They contain large-scale close folds plunging steeply southwestward and rest on peridotites with a subhorizontal tectonized contact offset locally by small steep faults. All specimens of peridotite that I have examined from this area are wholly serpentinized harzburgite, often with a compositional banding of originally orthopyroxene-poor and orthopyroxene-rich layers. Ricou (*1*) also concluded that the peridotite is harzburgite, although reporting a few specimens with up to 10 percent diallage. About 2 km from the westernmost skarn locality is an isolated hill (about 1 km^2 in area) of partly serpentinized, mylonitized, harzburgites and lherzolites.

The marble-peridotite contact truncates the folds in the marble blocks, and two groups of skarns are found within 30 m of it. Type 1 skarns occur within the serpentinized harzburgite, whereas type 2 skarns occur within the marbles. Type 1 skarns are clinopyroxenites and clinopyroxene-marbles. The pyroxenites resemble rodingite "dikes"; they are subparallel to the marble-serpentinite contact and are composed of coarse, equigranular, pale-green pyroxene with a few scattered grains of chrome spinel. The pyroxene-marbles occur as angular fragments up to 0.5 m in diameter containing only calcite and idioblastic, randomly oriented grains of pyroxene. Some fragments contain areas of undeformed, serpentinized harzburgite in which the contact between harzburgite and marble is marked by a zone (2 to 3 mm) of clinopyroxene partly altered to chlorite and calcite and completely undisturbed except where crosscut by later veins of calcite and chlorite. Type 2 skarns are subcircular wollastonite-pyroxene-calcite bodies up to 10 m in diameter. They are exposed on flat surfaces, and their three-dimensional form is unknown; they are very coarse-grained and have a granoblastic polygonal texture typical of high-temperature metamorphic rocks. Their contacts with the marbles are sharp, completely undisturbed, and marked locally by pegmatitic calcite. Garnet replaces wollastonite along some cleavage traces and grain boundaries, and adjacent dark-green pyroxene is patchily altered to a paler variety. Irregular subplanar zones crosscut the rocks in which plagioclase, garnet, and calcite are associated with poikilitic, altered pyroxene and wollastonite.

I interpret the field relations as in-

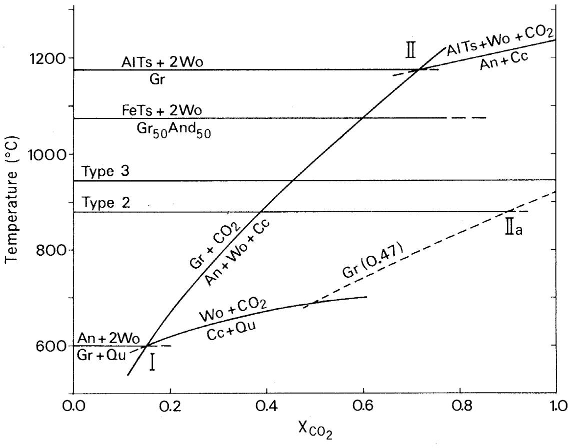

Fig. 1. A diagram of temperature versus fluid composition (T-X_{CO}) showing selected experimentally determined and calculated equilibria for the CaO-Al_2O_3-SiO_2-CO_2-H_2O and CaO-Fe_2O_3-SiO_2-CO_2-H_2O systems (*11*). Fluid pressure equals total pressure (2 kbar). The position of the isobaric invariant point I is experimentally determined (*11*), and the position of point II has been calculated from data in (*10*). The lines labeled type 2 and type 3 indicate the minimum temperatures for the reaction fassaite + wollastonite = garnet in the type 2 and type 3 skarns, estimated from the positions of the equilibria AlTs + 2Wo = Gr, and FeTs + 2Wo = $Gr_{50}And_{50}$ (*11*). The curve labeled Gr (0.47) indicates the shift of the curve Gr + CO_2 = An + Wo + Cc for grossular activity = 0.47, which is the maximum value for type 2 garnets; decreasing grossularite content of garnet will shift this curve to higher X_{CO_2} at constant temperature. The intersection of this curve with the type 2 line thus locates an isobaric invariant point (IIa), indicating a CO_2-rich fluid accompanying retrogression. Abbreviations: *AlTs*, aluminum Tschermak's pyroxene; *An*, anorthite; *And*, andradite; *Cc*, calcite; *FeTs*, ferric Tschermak's molecule (*6*); *Gr*, grossular; *Qu*, quartz; and *Wo*, wollastonite.

dicating that in most places little movement has occurred along an original intrusive contact. Type 2 skarns, which show no signs of tectonism at all, appear to represent originally intrusive "tongues" and are restricted to a zone within a few tens of meters of the present contact. The marbles often contain pyroxene close to the contact but not elsewhere. Type 1 skarns appear to represent part of a discontinuous zone at the marble-peridotite contact. Tectonism has resulted in the disruption of this rigid zone and produced a few centimeters of schistose serpentinite in places and has smoothed out most of the original irregularities of the contact and incorporated the type 1 skarns as blocks in serpentinite, although they remain close to their original position. In at least one place, an entire contact zone is apparently preserved undisturbed (*1*).

Another group of skarns (type 3) occurs discontinuously at the contacts between smaller marble blocks (less than 100 m in diameter) and serpentinite about 10 km east of Tang e Hana. These skarns have a coarse mylonitic foliation and contain fassaite, garnet, wollastonite, and anorthite porphyroclasts in a recrystallized matrix chiefly composed of wollastonite. They differ from types 1 and 2 in the much greater abundance of garnet and plagioclase and in the occurrence of sphene and apatite. These skarns are clearly not in their position of formation. Their contact with highly schistose serpentinite is sharp, and, although the mylonitic foliation is normally parallel to the serpentinite schistosity and the marble-serpentinite contact, in one place it is highly oblique to both. The mylonitization obviously predates the serpentinization since the fabric is overprinted by hydrous Ca-Al silicates typical of low-temperature calcium metasomatism associated with serpentinization. Intergrowth of fassaite and garnet in

Table 1. Representative analysis (oxide percent by weight), formulas, and end-members (mole percent) of coexisting minerals from skarns. Skarn types are indicated parenthetically. All samples were analyzed with an energy-dispersive electron microprobe with estimates of Fe_2O_3 for pyroxenes and garnets by assuming cation sums of 4 and 16 normalized to 6 and 24 oxygens, respectively. Wollastonite and plagioclase were recalculated to 6 and 32 oxygens, respectively. Analyses NY59-B6 and NY59-B9 are diopside and garnet formed by reaction of fassaite (NY59-B7) with wollastonite. For pyroxene end-members, see (*6*); for garnets, Gross = grossular, Andr = andradite, and Schorl = schorlomite; for plagioclase, An = anorthite and Ab = albite; N.D., not detected.

Sample	NY5-2 fassaite (type 1)	NY59-B7 fassaite (type 2)	NY59-B6 diopside (type 2)	NY59-B9 garnet (type 2)	NY59-1 wollastonite (type 2)	NY40-15 fassaite (type 3)	NY40-18 garnet (type 3)	NY40-13 plagioclase (type 3)	NY40-22 wollastonite (type 3)
SiO_2	47.37	45.68	52.64	38.02	51.54	41.77	37.69	44.41	51.31
TiO_2	0.73	0.93	0.02	1.09	N.D.	2.23	1.53	N.D.	N.D.
Al_2O_3	7.27	9.12	0.32	13.58	N.D.	12.27	13.05	35.78	N.D.
Fe_2O_3	4.34	4.59	0.79	11.64	0.00	3.86	11.73	N.D.	0.00
Cr_2O_3	0.30	0.04	N.D.	N.D.	N.D.	N.D.	N.D.	N.D.	N.D.
FeO	0.00	3.09	8.29	0.00	0.31	7.40	0.61	N.D.	0.35
MnO	N.D.	0.10	0.28	0.39	N.D.	N.D.	0.24	N.D.	N.D.
MgO	13.59	10.70	12.18	0.29	N.D.	7.72	0.44	N.D.	N.D.
CaO	25.42	25.28	25.46	35.82	48.32	24.04	34.95	19.36	47.87
Na_2O	0.24	0.18	0.13	N.D.	N.D.	N.D.	N.D.	0.48	N.D.
Total	99.26	99.71	100.11	100.83	100.17	99.29	100.25	100.03	99.53
Si	1.758	1.713	1.980	5.926	1.994	1.602	5.919	8.200	1.996
Al^{iv}	0.242	0.287	0.014	0.074	0.000	0.398	0.081	7.789	0.000
Al^{vi}	0.076	0.116	0.000	2.422	0.000	0.157	2.335	0.000	0.000
Ti	0.020	0.026	0.001	0.128	0.000	0.064	0.181	0.000	0.000
Fe^{3+}	0.121	0.130	0.022	1.365	0.000	0.111	1.386	0.000	0.000
Cr	0.009	0.001	0.000	0.000	0.000	0.000	0.000	0.000	0.000
Fe^{2+}	0.000	0.097	0.261	0.000	0.010	0.237	0.081	0.000	0.011
Mn	0.000	0.003	0.009	0.051	0.000	0.000	0.032	0.000	0.000
Mg	0.752	0.598	0.683	0.067	0.000	0.441	0.103	0.000	0.000
Ca	1.011	1.016	1.026	5.983	2.003	0.988	5.881	3.830	1.996
Na	0.017	0.013	0.009	0.000	0.000	0.000	0.000	0.172	0.000
	$AlTs_8$ $FeTs_{11}$ $TiTs_2$ $Others_{79}$	$AlTs_{12}$ $FeTs_{12}$ $TiTs_3$ $Others_{73}$	$AlTs_0$ $FeTs_1$ $TiTs_0$ $Others_{99}$	$Gross_{62}$ $Andr_{34}$ $Schorl_2$ $Others_2$		$AlTs_{16}$ $FeTs_{11}$ $TiTs_6$ $Others_{67}$	$Gross_{59}$ $Andr_{34}$ $Schorl_3$ $Others_4$	An_{96} Ab_4	

porphyroclasts and development of garnet rims on some porphyroclasts indicate that some of the mylonitization may have occurred during cooling and retrogression of the skarn assemblage soon after its formation.

Representative analyses of skarn minerals are listed in Table 1. Unaltered pyroxenes are characterized by high Ca, Al, and Fe^{3+} and low Na and are fassaites in which charge balance is maintained principally by the coupled substitutions

$$(Mg,Fe^{2+})Si \rightleftharpoons (Al,Fe^{3+})Al$$

and

$$(Mg,Fe^{2+})Si_2 \rightleftharpoons TiAl_2$$

in Tschermak's molecule [Ts, expressed as end-members AlTs, FeTs, and TiTs (*6*)]. Fassaites in the type 1 skarns (± calcite) have lower Ts contents than those in type 2 skarns (+ wollastonite + calcite), whereas type 3 fassaites (+ garnet + wollastonite + plagioclase) have the highest Ts contents. Garnets are grossular-andradite solid solutions with less than 10 mole percent of other end-members; those in type 2 skarns have a higher grossular content (57 to 70 mole percent) than those in type 3 skarns (42 to 59 mole percent). Plagioclase in type 2 skarns has altered to albite, epidote, and calcite but in type 3 skarns is anorthite-rich (89 to 97 mole percent). Wollastonite and calcite in all skarns are virtually pure.

Fassaite is found only in silica-poor, high-temperature environments (*7-9*) but has a relatively large stability field. However, the presence of wollastonite limits fassaite stability by reactions including:

$$\text{Ts} + \text{wollastonite} \rightarrow \text{garnet} \qquad (1)$$

Some constraint on formation temperatures for the skarn rocks is provided by the appearance of garnet, which is forming retrogressively by two reactions:

$$\text{Fassaite} + \text{wollastonite} \rightarrow \text{garnet} + \text{Ts-poor diopside} \qquad (2)$$

$$\text{Fassaite} + \text{wollastonite} + CO_2 \rightarrow \text{garnet} + \text{plagioclase} + \text{diopside} + \text{calcite} \qquad (3)$$

Temperatures for these reactions (Fig. 1) have been obtained from thermochemical data (*10*) and experimentally determined equilibria in the systems $CaO\text{-}Al_2O_3\text{-}SiO_2\text{-}H_2O$ (*11*) and $CaO\text{-}Al_2O_3\text{-}Fe_2O_3\text{-}SiO_2$ (*9*), and the effect of other components has been estimated (*11*). No equilibria directly fix pressure in the skarns, and therefore a total pressure of 2 kbar has been assumed by comparison with the stratigraphy of the nearby Oman ophiolite (*12*); fluid pressure has been assumed equal to total pressure. Reaction 2 is only slightly dependent on pressure (approximately 50°C/kbar, depending upon composition) and is independent of fluid composition; garnet-fassaite compositions indicate minimum temperatures at 2 kbar of 880°C for type 2 skarns and 920°C for type 3 skarns. The assemblage garnet-fassaite-wollastonite-plagioclase-calcite found in type 2 skarns as a result of reaction 3 fixes an isobaric invariant point (Fig. 1) in $T\text{-}X_{CO_2}$ space. Its position will vary slightly with varying Fe^{3+}/Al in fassaite and garnet, but, if it is assumed that plagioclase is pure anorthite similar to that in type 3 skarns (Table 1), the assemblage indicates a CO_2-rich fluid accompanying retrogression (Fig. 1).

These temperatures are minimum estimates for skarn formation (since they apply to retrograde reactions) and the very high estimated temperatures are supported by the type of fluid inclusions in fassaites and wollastonites of type 2 skarns. These contain primary and pseudo-secondary inclusions interpreted as magmatic inclusions, an indication that fassaite and wollastonite crystallized initially from a melt (*13*). Contact temperatures of at least 900°C therefore seem reasonable. Similar assemblages to those of the Neyriz skarns have been reported from dolomitic limestone xenoliths at the margin of the Bushveld lopolith for which intrusion temperatures of the order of 1100°C have been suggested (*9, 14*); differences in mineral assemblages are a reflection of the initial Mg-poor composition of the Neyriz marbles. Fassaite-garnet assemblages produced from limestones metamorphosed by gabbros of the Boulder batholith (*8*) appear to differ not only in bulk composition and fluid composition but were metamorphosed at rather lower temperatures, as indicated by the absence of the assemblage garnet-fassaite-wollastonite (*15*).

The only reasonable explanation for the origin of these high-temperature skarns is the intrusion of the ophiolite peridotite. Metamorphism of the peridotite can be excluded because of the absence of any signs of metamorphism, other than the later episode of serpentinization, and the large amounts of introduced Ca and CO_2 required. Calcium metasomatism has occurred but has produced a characteristic set of minerals including pectolite, prehnite, grossular, hydrogrossular, Ts-poor diopside, and chlorite. These minerals clearly postdate skarn formation and retrogression and are typical of low-temperature Ca-metasomatism associated with serpentinization (*16*). Regional metamorphism of impure limestones fails to explain the consistent and intimate spatial relationships between peridotite, skarn, and marble; the very high temperatures required would also be extremely unusual. The present structural position of the skarns on top of the peridotite and their mineralogy and textures are very different to subophiolite metamorphic rocks (*17*) produced by obduction. The type 3 skarns are not in their position of formation and could be explained as remnants of a contact with the ophiolite gabbros now exposed within a few kilometers of the easternmost skarn localities. This would explain their relatively high Al, Ti, and P contents. However, skarns are never found associated with the gabbros, and the mineralogical and chemical similarities to type 1 and type 2 skarns, which are clearly related to the peridotite, suggest a similar origin for the type 3 skarns. The zonation reported from a complete contact (*1*) suggests that the type 3 skarns represent the remnant of a skarn zone closest to the peridotite. There are no other intrusive rocks in the Neyriz region which could have been responsible for the skarn formation.

The evidence therefore indicates that the skarns formed partly by crystallization of a melt formed at the contact and partly by diffusion metasomatism, as a result of the intrusion of peridotite into continental basement limestones. This origin of the crystalline limestones is suggested by the large-amplitude folds crosscut by the peridotite contact. The peridotite may have been intruded as a crystal mush with a small amount of partial melt produced by adiabatic melting induced by sudden continental rifting, or it may have been hot and solid but plastic and locally molten at the contact as a result of the introduction of CO_2. In a CO_2-rich fluid phase SiO_2, Al_2O_3, Fe_2O_3, CaO, and MgO were probably the chief components (*18*), but the skarn zone formed would probably have been narrow since the energy required for the assimilation of marble is supplied largely by the enthalpy of crystallization of phases from the magma (*18, 19*). Formation of skarn minerals would therefore have accelerated the cooling and crystallization of the intrusion. In such a case, the composition of the pyroxene would be a function of the rates of diffusion and chemical potential gradients across the contact during multicomponent diffusion. The increasing Ts content of the fassaite from type 1 to type 3 skarns is a consequence of the higher diffusion rates and higher initial concentrations in the peridotite of

SiO_2 and MgO compared to Al_2O_3 and Fe_2O_3. Zoning of the pyroxenes is not observed and is unlikely to be preserved since intracrystalline diffusion is much more effective at high temperatures.

The preservation of an intrusive contact is therefore more consistent with models of the Neyriz ophiolite, that suggest an origin during continental rifting (*20*) (perhaps resulting in an ocean similar to the present-day Red Sea) rather than at the spreading center of a wide ocean destroyed through subduction (*5*) or partially obducted as a hot slab (*4*). Other ophiolites of the Tethyan belt, where evidence for subduction and obduction is often weak, may have originated in a similar manner.

ROBERT HALL

Department of Geological Sciences
Queen Mary College, University of
London, London E1 4NS, England

References and Notes

1. L.-E. Ricou, *Bull. Soc. Geol. Fr.* **13**, 146 (1971).
2. K. W. Gray, *Q. J. Geol. Soc. London* **105**, 189 (1949).
3. A. J. Wells, *Geol. Mag.* **106**, 385 (1969).
4. N. H. Woodcock and A. H. F. Robertson, *Geology* **5**, 373 (1977).
5. S. J. Haynes and H. McQuillan, *Geol. Soc. Am. Bull.* **85**, 739 (1974).
6. Pyroxene end-members have been calculated in the order suggested by H. S. Yoder and C. E. Tilley [*J. Petrol.* 3, 342 (1962)]. Sodium has been assigned to acmite ($NaFe^{3+}Si_2O_6$), and Tschermak's molecule (Ts) has been calculated as three end-members, aluminum Ts (AlTs, $CaAl_2SiO_6$), ferric Ts (FeTs, $CaFe^{3+}AlSiO_6$), and titanium Ts (TiTs, $CaTiAl_2O_6$).
7. W. A. Deer, R. A. Howie, J. Zussman, *Rock-Forming Minerals* (Longmans, London, 1978); C. E. Tilley, *Geol. Mag.* **75**, 81 (1938).
8. A. Knopf and D. E. Lee, *Am Mineral.* **42**, 73 (1957).
9. H. G. Huckenholz, W. Lindhuber, J. Springer, *Neues Jahrb. Mineral. Abh.* **121**, 160 (1974).
10. H. C. Helgeson, J. M. Delany, H. W. Nesbitt, D. K. Bird, *Am. J. Sci.* **278A**, 1 (1978).
11. Experimentally determined equilibria are as follows: (i) calcite + quartz = wollastonite + CO_2 [H. J. Greenwood, *Am. Mineral.* **52**, 1669 (1967)]; (ii) calcite + anorthite + wollastonite = grossular + CO_2 [T. M. Gordon and H. J. Greenwood, *ibid.* **56**, 1674 (1971)]; (iii) anorthite + 2 wollastonite = grossular + quartz [A. L. Boettcher, *J. Petrol.* **11**, 337 (1970)]; (iv) $grossular_{50}andradite_{50}$ = FeTs + 2 wollastonite (*9*). The position of the invariant point I (Fig. 1) has been taken as 600°C and $X_{CO_2} = 0.15$. The positions of other equilibria have been calculated from data in (*10*). The effect of other components has been estimated: for garnet, by assuming an ideal solution model [J. Ganguly, *Contrib. Mineral. Petrol.* **55**, 81 (1976)]; for fassaite, by assuming that AlTs activity = X_{AlTs}, which is consistent with experimentally determined activity-composition relations for Di-Hd-AlTs (Di is diopside, and Hd is hedenbergite) solid solutions with $X_{AlTs} < 0.3$ [B. J. Wood, *Am. Mineral.* **61**, 599 (1976)] and assuming that FeTs activity = X_{FeTs}. The activities of plagioclase, wollastonite, and calcite have been taken as unity.
12. B. M. Reinhardt, *Schweiz, Mineral. Petrogr. Mitt.* **49**, 1 (1969).
13. Complex inclusions ranging in size from a few microns to ≃ 20 μ are common in the pyroxenes as planar groupings traversing the host crystal but do not continue into the adjacent wollastonite, and they are therefore classed as pseudosecondary inclusions. Similar, but isolated, inclusions occur and are interpreted as primary. The inclusions commonly contain more than 50 percent crystalline material and a low-density vapor phase which rarely has a rim of liquid. Some of the crystalline material appears to be calcite. Similar, though less common, inclusions occur in wollastonite. All these inclusions are interpreted as magmatic inclusions, an indication that fassaite and wollastonite crystallized from a melt.
14. J. A. Willemse and J. J. Bensch, *Trans. Geol. Soc. S. Afr.* **67**, 1 (1964).
15. R. J. Shedlock and E. J. Essene, *J. Petrol.* **20**, 71 (1979).
16. R. G. Coleman, *Bull. U.S. Geol. Surv. 1247* (1967).
17. _____, *Ophiolites: Ancient Oceanic Lithosphere* (Springer Verlag, Berlin, 1977); H. Williams and W. R. Smyth, *Am. J. Sci.* **273**, 594 (1973); J. Zimmerman, *Geol. Soc. Am. Mem. 132* (1972), p. 225.
18. R. Joesten, *Geol. Soc. Am. Bull.* **88**, 1515 (1977).
19. N. L. Bowen, *The Evolution of the Igneous Rocks* (Princeton Univ. Press, Princeton, N.J., 1928); D. H. Watkinson and P. J. Wyllie, *Geol. Soc. Am. Bull.* **80**, 1565 (1969).
20. R. Stoneley, *Tectonophysics* **25**, 303 (1975).
21. I thank M. Arvin for the opportunity to visit Neyriz and H. S. Edgell for help with fieldwork. I thank P. Suddaby, N. Wilkinson, and K. Brodie, who provided assistance with microprobe analyses carried out in the Geology Department, Imperial College, London. I thank A. H. Rankin for examination and interpretation of the fluid inclusions and M. G. Audley-Charles and W. J. French for discussions.

3 December 1979; revised 14 March 1980

Aragonite Twinning in the Molluscan Bivalve Hinge Ligament

Abstract. *Molluscan bivalve hinge ligaments are composed of long needle-shaped aragonite crystals embedded in a protein matrix. These crystals are twinned and, in general, the twin forms a thin lamella through the center of the crystal.*

By electron microscopy and electron diffraction of single crystals in thin sections, we have demonstrated that the aragonite ($CaCO_3$) crystals in the molluscan bivalve hinge ligament are twinned. Aragonite is orthorhombic belonging to space group *Pmcn*. Inorganic sources of the mineral are commonly observed to be twinned about the (110) morphologic plane (*1*). Thin twin lamellae have been observed in electron micrographs of aragonite crystals from limestone deposits (*2*). Our experiments are apparently the first demonstration of twinning in biogenic aragonite, although Mutvei (*3*) has proposed that, on the basis of crystal morphology alone, the aragonite crystals of bivalve shell nacre are twinned.

The bivalve hinge ligament is composed of long needle-shaped aragonite crystals embedded in an elastic, predominantly protein matrix (*4*). The crystals are pseudohexagonal in cross section (Fig. 1), and the morphologically long (crystallographic *c*) axis is oriented perpendicular to the growing margin of the ligament. The crystals are about 100 nm in cross section. For electron microscopy, 0.5-mm slices of the ligament were fixed in 5 percent glutaraldehyde in 0.1*M* cacodylate buffer, *p*H 7.6, for 4 hours, then dehydrated with ethanol and embedded in Epon. With a dry diamond knife, 100-nm sections were cut perpendicular to the *c* axis of the crystals. The sections were transferred to a water surface with a fine hair and picked up immediately on copper grids to prevent dissolution of the crystals. Images and diffraction data were obtained with a Philips 200 electron microscope. Images were recorded at 60 kV and diffraction data at 100 kV.

The electron micrographs of *Mya arenaria* and *Spisula solidissima* (Fig. 1) show hinge ligament cross sections. The electron-opaque structures are the aragonite crystals; the electron lucent area is the organic matrix. Since the *c* axes of the individual crystals (which are nearly perpendicular to the plane of the micrographs) are not perfectly parallel, not all of the crystals in a section are in a reflecting orientation. Those crystals that are in a strongly reflecting orientation have opaque images as a result of

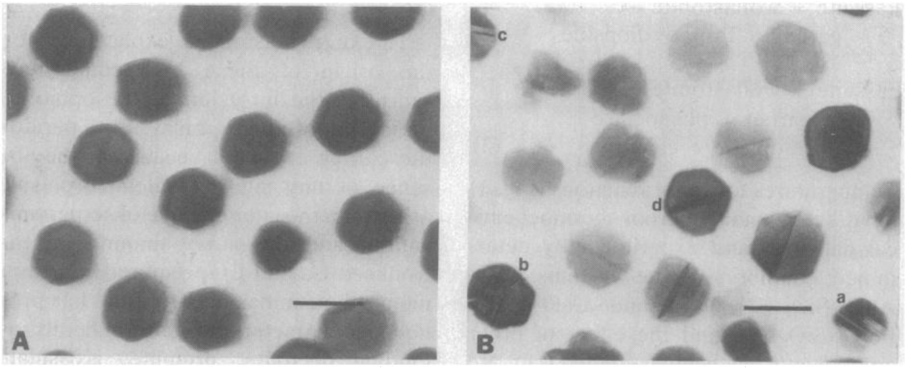

Fig. 1. Electron micrographs of hinge ligaments showing the aragonite crystals in cross section. (A) The *Mya arenaria* ligament. The thin bands through the center of the crystals are thin twin lamellae. (B) The *Spisula solidissima* ligament. Crystal *a* has multiple twin lamellae and crystal *b* has twin lamellae on both the (110) and ($1\bar{1}0$) planes. Crystal *c* has a thick twin lamella and the lower third of crystal *a* is in the twin orientation. Bar equals 100 nm.

0036-8075/80/0613-1262$00.50/0 Copyright © 1980 AAAS